New Universality Class Describes Vicsek's Flocking Phase in Physical Dimensions

Patrick Jentsch and Chiu Fan Lee*
Department of Bioengineering, Imperial College London, South Kensington Campus, London SW7 2AZ, United Kingdom

(Received 4 March 2024; accepted 5 August 2024; published 17 September 2024)

The Vicsek simulation model of flocking together with its theoretical treatment by Toner and Tu in 1995 were two foundational cornerstones of active matter physics. However, despite the field's tremendous progress, the actual universality class (UC) governing the scaling behavior of Viscek's "flocking" phase remains elusive. Here, we use nonperturbative, functional renormalization group methods to analyze, numerically and analytically, a simplified version of the Toner-Tu model, and uncover a novel UC with scaling exponents that agree remarkably well with the values obtained in a recent simulation study by Mahault *et al.* [Phys. Rev. Lett. **123**, 218001 (2019)], in *both* two and three spatial dimensions. We therefore believe that there is strong evidence that the UC uncovered here describes Vicsek's flocking phase.

DOI: 10.1103/PhysRevLett.133.128301

Two papers in 1995 arguably led to the advent of active matter physics, which has in many ways revolutionized nonequilibrium, soft matter, and biological physics. Reference [1] studied the order-disorder transition of an active XY model in two dimensions (2D) using a simulation model now commonly known as the Vicsek model. Inspired by the existence of the ordered flocking phase, which is forbidden in equilibrium systems by the Mermin-Wagner-Hohenberg theorem, Toner and Tu introduced a set of hydrodynamic equations of motion (EOM) for generic polar active fluids in Ref. [2], now known as the Toner-Tu (TT) model. Their renormalization group (RG) analysis of these equations lead to nontrivial scaling behaviour associated to this phase. Intriguingly, controversies soon emerged regarding these two landmark studies: the *critical* order-disorder transition, the focus of Ref. [1], was found to be preempted by a discontinuous phase transition [3]; and the RG study performed in Ref. [2] was found to be incomplete due to neglected nonlinearities in the original analysis [4]. More recently, an extensive simulation study [5] of Vicsek's flocking phase has provided estimates for the scaling exponents that deviate significantly from the original predictions of Ref. [2]. As a result, the question of *what universality class (UC) actually describes Vicsek's flocking phase* remains open. Indeed, a solution has been widely considered to be intractable using current RG methodology due to its inherent complexity [4].

*Contact author: c.lee@imperial.ac.uk

Published by the American Physical Society under the terms of the Creative Commons Attribution 4.0 International license. Further distribution of this work must maintain attribution to the author(s) and the published article's title, journal citation, and DOI.

Here, we made a significant step forward in tackling the above question using a functional renormalization group (FRG) [6–14] analysis. Specifically, we introduce a simplified model that reveals for the first time the crucial impact of the compressibility of active fluids to the scaling behavior in the flocking phase. The FRG analysis of our model leads to a set of scaling relations that enable us to solve for the three scaling exponents: the roughness exponent (χ), dynamic exponent (z), and anisotropy exponent (ζ), which characterize the UC of the flocking phase.

Using the rescaling convention,

$$(t, \mathbf{r}_\perp, x, \delta\mathbf{g}, \delta\rho) \to (te^{zl}, \mathbf{r}_\perp e^{l}, xe^{\zeta l}, \delta\mathbf{g}e^{\chi l}, \delta\rho e^{\chi l}), \quad (1)$$

where, without loss of generality, the flocking direction is chosen to be along the x axis, these novel exponents are

$$\chi = \frac{13(1-d)}{40}, \qquad z = \frac{27+13d}{40}, \qquad \zeta = \frac{41-d}{40}, \quad (2)$$

for $d < 11/3$ where d is the spatial dimension. Remarkably, the values of these exponents agree very well with the simulation results in *both* two and three dimensions (falling within the given simulation errors, see Table I). Therefore, we believe that the new UC uncovered here describes the ordered phase of the Vicsek model.

Simplified Toner-Tu model—We start with the celebrated TT EOM that describe generic compressible polar active fluids, derived simply from considering the underlying conservation law and symmetries of the system [2,4,15]:

$$\partial_t \rho + \nabla \cdot \mathbf{g} = 0, \quad (3)$$

TABLE I. Comparison of the scaling exponents obtained here [Eqs. (2)], from a simulation study of the Vicsek model [5], from the Toner-Tu 1995 paper [2], and from dynamic renormalization group analyses of two closely related models: the *incompressible* TT model [16–18] and the *Malthusian* version of the TT model [19,20].

Spatial dimension (d)	χ	z	ζ
$d = 2$:			
This letter	−0.325	1.325	0.975
Vicsek simulation [5]	−0.31(2)	1.33(2)	0.95(2)
Incompressible [16,17]	−0.23	1.1	0.67
TT 95 / Malthusian [2,19]	−0.20	1.20	0.6
$d = 3$:			
This letter	−0.65	1.65	0.95
Vicsek simulation [5]	−0.62	1.77	1
TT 95 / incompressible [2,18]	−0.60	1.60	0.8
Malthusian [20]	−0.45(2)	1.45(2)	0.73(1)

$$\partial_t \mathbf{g} + \lambda_1(\mathbf{g}\cdot\nabla)\mathbf{g} + \lambda_2\mathbf{g}(\nabla\cdot\mathbf{g}) + \frac{\lambda_3}{2}\nabla(|\mathbf{g}|^2) = -U\mathbf{g} + \mu_1\nabla^2\mathbf{g} + \mu_2\nabla(\nabla\cdot\mathbf{g}) + \mu_3(\mathbf{g}\cdot\nabla)^2\mathbf{g} - \nabla P_1 - \mathbf{g}(\mathbf{g}\cdot\nabla)P_2 + \text{h.o.t.} + \mathbf{f} + \mathbf{Q}, \quad (4)$$

where ρ is the mass density field and $\mathbf{g}$ is the momentum density field. Note that instead of using the velocity density field as one of the two hydrodynamic variables in the original formulation [2,15], we have opted for the momentum density field. The physics of course remains the same but this choice has the virtue of simplifying the continuity equation (3) by rendering it linear. In the EOM of $\mathbf{g}$ (4), all coefficients are generic functions of ρ and $|\mathbf{g}|$, and the "flocking-inducing" term U is such that $U < 0$ if $|\mathbf{g}| < g_0$ while $U > 0$ if $|\mathbf{g}| > g_0$ for some mean momentum density magnitude g_0, thus leading to a nonzero preferred momentum density. The "pressure" terms P_1 and P_2 are functions of ρ:

$$P_1 = \sum_{n\geq 1}\kappa_n(\rho-\rho_0)^n, \qquad P_2 = \sum_{n\geq 1}\nu_n(\rho-\rho_0)^n, \quad (5)$$

where ρ_0 is the mean density, and the coefficients κ_n's and ν_n's are themselves functions of $|\mathbf{g}|$. Furthermore, "h.o.t." in Eq. (4) denotes higher order terms in spatial derivatives (e.g., $\nabla^4\mathbf{g}$, etc.) that are irrelevant to our discussion, and the noise term $\mathbf{f}$ is Gaussian with vanishing mean and statistics:

$$\langle f_i(\mathbf{r},t)f_j(\mathbf{r}',t')\rangle = 2D\delta_{ij}\delta^{d+1}(t-t',\mathbf{r}-\mathbf{r}'). \quad (6)$$

Finally, in addition to the usual terms, we have also introduced the Lagrange multiplier $\mathbf{Q}$ in Eq. (4) to enforce that the fluctuations in $\mathbf{g}$ along the flocking direction $\delta\mathbf{g}_x$ vanish (*Simplification 1*). This simplification is inspired by the equilibrium $O(N)$ model [21–23] and the incompressible TT model [18,24], where the fluctuations $\delta\mathbf{g}_x$ can be neglected without affecting the UC of the Goldstone modes since they are subleading in the hydrodynamic limit. Specifically, introducing a similar simplification in the $O(N)$ model or the incompressible TT theory produces exactly the same RG equations for the Goldstone mode as if $\delta\mathbf{g}_x$ had been simply neglected, i.e., the UC of the Goldstone mode remains unchanged. However, we note that this simplification does alter the physics of the remaining modes. In the standard $O(N)$ or incompressible TT theory, the modulus of $\mathbf{g}$ becomes truly massive in the hydrodynamic limit, while the $\delta\mathbf{g}_x$ mode becomes soft to compensate fluctuations of the Goldstone mode. In the presence of the Lagrange multiplier, $\delta\mathbf{g}_x = 0$ exactly and can therefore not compensate these fluctuations. As a result, the modulus $|\mathbf{g}|$ becomes a soft variable. Simplification 1 is therefore distinct from a nonlinear sigma model constraint. If one constrains the modulus $|\mathbf{g}|$ (as in the nonlinear sigma model), the Goldstone modes have generically a more complicated angular dependence [4]; while simplification 1 (employed here) produces a very simple angular dependence, rendering the numerical solution of the FRG equations achievable. In both cases, the linear scaling exponents are the same and, judging by the nonlinear exponents obtained using our approach (Table I), the nontrivial UC may also be unchanged by our simplification 1.

Besides simplification 1, we will reduce the complexity further by ignoring all nonlinearities in the TT EOM involving the density field (*Simplification 2*), corresponding to the limit of small density fluctuations. This simplification is motivated by the successes in previous studies of variants of the TT model where the density field is neglected completely, thus rendering the model analytically tractable [16–20]. However, as noted before, these previous approaches are not sufficient to describe the scaling exponents observed in simulations (see Table I). In contrast, the density and momentum fields are still coupled at the linear level in our model, which, as we shall see, leads to novel emergent hydrodynamic behavior.

Linear theory—In the flocking phase, the mean magnitude of the momentum field, $g = |\mathbf{g}|$, is nonzero and we are interested in the fluctuating fields around this flocking state:

$$\delta\rho = \rho - \rho_0, \qquad \delta\mathbf{g} = \mathbf{g} - g_0\hat{\mathbf{x}}, \quad (7)$$

where hats denote normalized vectors. We now further partition $\delta\mathbf{g}$ into three components that are more natural in our analysis: $\delta\mathbf{g} = \delta\mathbf{g}_x + \delta\mathbf{g}_L + \delta\mathbf{g}_T$, where $\delta\mathbf{g}_x = \hat{\mathbf{x}}(\hat{\mathbf{x}}\cdot\delta\mathbf{g})$, $\delta\mathbf{g}_L = \hat{\mathbf{q}}_\perp(\hat{\mathbf{q}}_\perp\cdot\delta\mathbf{g})$, and $\mathbf{q}_\perp$ denotes the wave vector (in spatially transformed Fourier space) perpendicular to the $\mathbf{x}$ direction, i.e., $\mathbf{q}_\perp = \mathbf{q} - q_x\hat{\mathbf{x}}$ and $q_x = \hat{\mathbf{x}}\cdot\mathbf{q}$. Namely, the three components of $\delta\mathbf{g}$ correspond to its component along the flocking direction, along the direction of the wave vector (with the $\mathbf{x}$-component

subtracted), and along the direction perpendicular to both wave vector and flocking direction. Note that simplification 1 enforces that $\delta\mathbf{g}_x = 0$ here.

We now analyze the scaling behavior of the ordered phase at the linear level, i.e., by first truncating the TT EOM to linear order in $\delta\rho$, $\delta\mathbf{g}_L$, and $\delta\mathbf{g}_T$. The propagators can be obtained by inverting the "dynamical matrix" constructed from the linear TT EOM [25]:

$$\mathbf{G}(\tilde{\mathbf{q}}) = \mathbf{G}_L(\tilde{\mathbf{q}}) + \mathbf{G}_T(\tilde{\mathbf{q}}), \tag{8}$$

$$\mathbf{G}_L(\tilde{\mathbf{q}}) = \frac{-\mathrm{i}\omega_q \mathcal{P}_L(\mathbf{q})}{-\mathrm{i}\omega_q(-\mathrm{i}\omega_q + \mathrm{i}\lambda_g q_x + \mu_x q_x^2 + \mu_\perp^L q_\perp^2) + \kappa_1 q_\perp^2}, \tag{9}$$

$$\mathbf{G}_T(\tilde{\mathbf{q}}) = \frac{\mathcal{P}_T(\mathbf{q})}{-\mathrm{i}\omega_q + \mathrm{i}\lambda_g q_x + \mu_x q_x^2 + \mu_\perp q_\perp^2}, \tag{10}$$

where we have defined $\tilde{\mathbf{q}} = (\omega_q, \mathbf{q})$, $q_\perp = |\mathbf{q}_\perp|$, and the projectors $\mathcal{P}_{L,ij}(\mathbf{q}) = \hat{q}_{\perp,i}\hat{q}_{\perp,j}$ and $\mathcal{P}_{T,ij}(\mathbf{q}) = \delta_{ij} - \hat{x}_i\hat{x}_j - \hat{q}_{\perp,i}\hat{q}_{\perp,j}$. Further we have defined $\lambda_g = \lambda_1 g_0$, $\mu_\perp = \mu_1$, $\mu_x = \mu_1 + \mu_3 g_0^2$, and $\mu_\perp^L = \mu_1 + \mu_2$, which are all evaluated at $\delta\rho = \delta\mathbf{g} = 0$. Since $\delta\mathbf{g}_x = 0$, $\mathbf{G}$ is perpendicular to $\hat{\mathbf{x}}$.

The equal-time correlation functions can now be obtained in the usual way, giving,

$$\langle \delta\mathbf{g}_L(t,\mathbf{r})\delta\mathbf{g}_L(t,0)\rangle = D\int_{\mathbf{q}} e^{-\mathrm{i}\mathbf{q}\cdot\mathbf{r}} \frac{\mathcal{P}_L(\mathbf{q})}{\mu_x q_x^2 + \mu_\perp^L q_\perp^2}, \tag{11}$$

$$\langle \delta\mathbf{g}_T(t,\mathbf{r})\delta\mathbf{g}_T(t,0)\rangle = D\int_{\mathbf{q}} e^{-\mathrm{i}\mathbf{q}\cdot\mathbf{r}} \frac{\mathcal{P}_T(\mathbf{q})}{\mu_x q_x^2 + \mu_\perp q_\perp^2}, \tag{12}$$

$$\langle \delta\rho(t,\mathbf{r})\delta\rho(t,0)\rangle = \frac{D}{\kappa_1}\int_{\mathbf{q}} e^{-\mathrm{i}\mathbf{q}\cdot\mathbf{r}} \frac{1}{\mu_x q_x^2 + \mu_\perp^L q_\perp^2}, \tag{13}$$

where $\int_{\mathbf{q}} = \int d^d\mathbf{q}/(2\pi)^d$. In particular, our linear analysis identifies the following scaling exponents $\chi_\rho^{\mathrm{lin}} = \chi^{\mathrm{lin}} = (2-d)/2$, $z^{\mathrm{lin}} = 2$ and $\zeta^{\mathrm{lin}} = 1$ which, as expected, are identical to those in previous works [2,4,15].

Nonlinear analysis using FRG—Applying simplification 2 to eliminate all nonlinearities involving $\delta\rho$, the only nonlinearities left are terms involving the λ's and U, which become independent of $\delta\rho$. The standard power counting method (e.g., see [27]) shows that below $d = 4$, the leading order contributions of these nonlinearities (i.e., the λ's, which are no longer functions of $\delta\mathbf{g}$, and $U = \beta|\delta\mathbf{g}|^2/2$) can modify the scaling behavior and thus have to be incorporated into the analysis. RG methods provide a systematic way to accomplish this task and we will use here the functional version of the renormalization group based on the *exact* Wetterich equation [7–9]:

$$\partial_k \Gamma_k = \frac{1}{2}\mathrm{Tr}\left[\left(\Gamma_k^{(2)} + R_k\right)^{-1}\partial_k R_k\right], \tag{14}$$

where Γ_k is the wavelength (k) dependent effective average action and R_k is a regulator that serves to control the length scale ($\sim 1/k$) beyond which fluctuations are averaged over. The exact flow equation (14) serves to interpolate between the microscopic action Γ_Λ (where all model details are encoded) and the macroscopic effective average action Γ_0, from which the EOM for the *averages* of the fields can be obtained. The trace is a sum over all degrees of freedom, i.e., over all field indices, wave vectors, and frequencies, and $\Gamma_k^{(2)}$ is the matrix containing the second order functional derivatives of Γ_k with respect to the fields. The boundary conditions for Γ_k described above are enforced by requiring that $R_\Lambda \sim \infty$ and $R_0 = 0$.

To proceed with our FRG analysis, we use the Martin-Siggia-Rose-de Dominicis-Janssen formalism [14,28–30] by introducing the response fields $\bar{\mathbf{g}}_\perp$ and $\bar{\rho}$, to obtain a scalar action Γ_Λ that describes our theory at the microscopic scale Λ. Making all microscopic couplings dependent on k (not written explicitly), we obtain an ansatz for the scale-dependent effective average action,

$$\Gamma_k[\bar{\mathbf{g}}_\perp, \mathbf{g}_\perp, \bar{\rho}, \rho] = \int_{\tilde{\mathbf{r}}} \Big\{ \bar{\rho}[\partial_t\rho + \nabla_\perp\cdot\mathbf{g}_\perp] - D|\bar{\mathbf{g}}_\perp|^2 + \bar{\mathbf{g}}_\perp\cdot\Big[\gamma\partial_t\mathbf{g}_\perp + \lambda_1 g_0\partial_x\mathbf{g}_\perp + \lambda_1(\mathbf{g}_\perp\cdot\nabla_\perp)\mathbf{g}_\perp + \lambda_2\mathbf{g}_\perp(\nabla_\perp\cdot\mathbf{g}_\perp) + \frac{1}{2}\lambda_3\boldsymbol{\nabla}_\perp(|\mathbf{g}_\perp|^2) + \frac{1}{2}\beta|\mathbf{g}_\perp|^2\mathbf{g}_\perp - \mu_1\nabla_\perp^2\mathbf{g}_\perp - \mu_1\partial_x^2\mathbf{g}_\perp - \mu_2\nabla_\perp(\nabla_\perp\cdot\mathbf{g}_\perp) - \mu_3 g_0^2\partial_x^2\mathbf{g} + \kappa_1\nabla\rho\Big]\Big\}, \tag{15}$$

where we have defined $\mathbf{g}_\perp = \delta\mathbf{g}_L + \delta\mathbf{g}_T$ and $\int_{\tilde{\mathbf{r}}} = \int d^d\mathbf{r}dt$. We have also introduced the coefficient γ to allow for the potential renormalization of the time-derivative term. Because of its linear structure, the "density sector" (proportional to $\bar{\rho}$) does not get renormalized [31,32], and therefore its coefficients remain unity.

The last ingredient in the FRG formulation is the regulator, which we choose to be [33],

$$R_k(\tilde{\mathbf{q}}, \tilde{\mathbf{p}}) = \Gamma_k^{(2)}(\tilde{\mathbf{q}}, \tilde{\mathbf{p}})\left(\frac{1}{\Theta_\epsilon(q_\perp - k)} - 1\right), \tag{16}$$

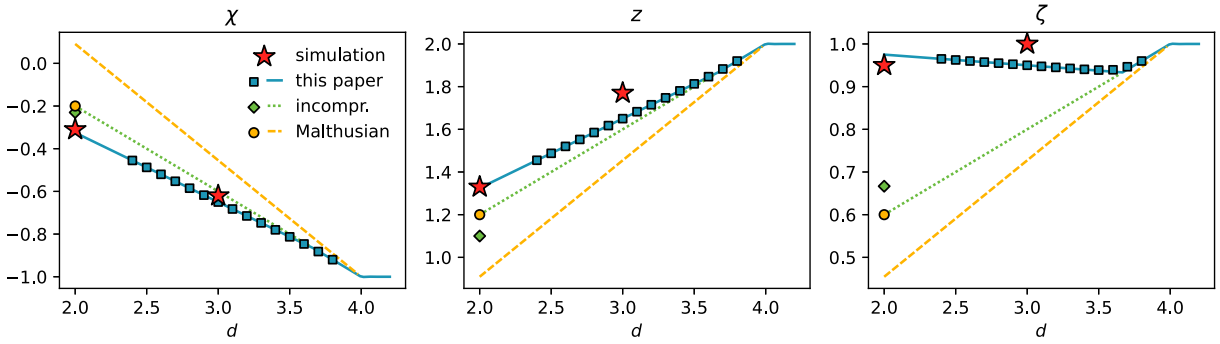

FIG. 1. Exponents, χ, z, and ζ, obtained from our analytical results (2) (unbroken blue line) and our numeric RG calculation (blue squares) show good agreement with the simulation results of Vicsek's flocking phase (red stars) [5]. For comparison, scaling exponents of the incompressible TT model (green dotted line for $d > 2$ [18] and green diamond for $d = 2$ [16,17]) and those of the Malthusian (or infinitely compressible) TT model (yellow dashed lines for $d > 2$ [20], yellow circle for $d = 2$ [19]) are also shown. Note that the results from the Toner-Tu 1995 paper [2] coincide with the dotted green line and the yellow circle.

where Θ_ϵ is a smooth, nonzero function that approaches the Heaviside function in the limit of $\epsilon \to 0$, which is to be taken at the end of the calculation. Our choice of regulator leads to the $q_\perp$ integral in the graphical corrections to become a trivial integral over a delta function. This is numerically advantageous as we then only need to evaluate the q_x integral numerically, instead of having to perform a two-dimensional integral. We further note that since the regulator has the same structure as the propagator, even though it is frequency dependent, causality is preserved [14].

RG fixed points—With the regulator and ansatz defined, we can now deduce the flow equations, for which we rely on computer algebra due to the complexity of the propagators and interaction terms. Further details are given in Ref. [25].

Integrating the flow equations numerically, we always find a nontrivial stable fixed point. The associated scaling exponents are shown in Fig. 1 (blue squares). For dimensions $11/3 \lesssim d < 4$, the scaling exponents agree with those obtained by Toner and Tu in Refs. [2,15]:

$$\chi^{\mathrm{TT}} = \frac{3-2d}{5}, \qquad z^{\mathrm{TT}} = \frac{2(d+1)}{5}, \qquad \zeta^{\mathrm{TT}} = \frac{d+1}{5}. \tag{17}$$

Intriguingly, below $d \approx 11/3$, the values of the exponents are found to agree with the new formula shown in Eq. (2), until for $d \lesssim 2.4$ when the RG flow seems to become divergent. We hypothesize that the divergence is due to our truncation or simplification of the scale-dependent average action, as we reason that the density-dependent couplings could become more important in lower dimensions and potentially stabilize the RG flow.

We interpret our findings as follows. The flocking phase of our simplified TT model is generically described by the TT UC for $11/3 < d < 4$. Below $d < 11/3$, a new stable RG fixed point, with scaling behavior given by Eq. (2), emerges. And comparing the values of the exponents obtained using Eq. (2) to a recent simulation study [5] (red stars in Fig. 1), we believe that the UC uncovered here describes the ordered phase of the Vicsek model. Schematics of the RG flows illustrating the stability exchange between the TT UC and the UC described here are shown in Fig. 2 in terms of the anomalous dimensions $\eta_\perp$ and η_x, defined as the graphical corrections of $\mu_\perp$ and μ_x,

$$\partial_l \log \mu_\perp = z - 2 + \eta_\perp, \tag{18}$$

$$\partial_l \log \mu_x = z - 2\zeta + \eta_x. \tag{19}$$

Analytical treatment—We will now go beyond our numerical FRG calculation by using an analytical approach, whose advantage is threefold: (i) to obtain analytical expressions of the scaling exponents (2) beyond relying

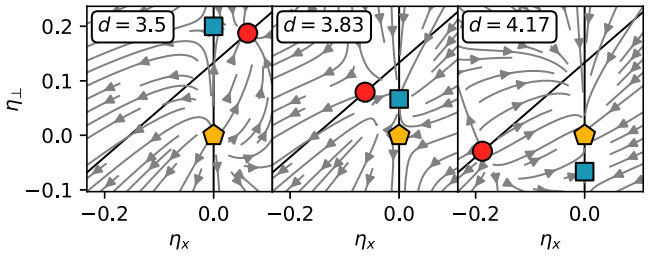

FIG. 2. Schematic flow diagram visualizing the locations and stability of the Gaussian (yellow pentagon), the TT (blue square) and the novel compressible fixed points (red circle) in the $(\eta_x, \eta_\perp)$ plane for dimensions below $d_c' = 11/3$, in between d_c' and $d_c = 4$, and above d_c. The flow diagrams in the physical dimensions 2 and 3 are topologically equivalent to the left diagram at $d = 3.5$. $\eta_\perp$ and η_x are the graphical corrections of $\mu_\perp$ and μ_x, respectively (18), (19). The black lines are the fixed point trajectories as d is increased. The gray flow lines are fictitious and serve to illustrate the stability of the fixed points, as verified by our numerical FRG calculation.

on fitting the numerical results; (ii) to understand why the values of the exponents seem to be quantitatively accurate in $d = 2$, 3, as compared to simulations, even with drastic truncations or approximations adopted, and (iii) to verify the exchange of stability between the TT UC and our new UC at $d \approx 11/3$.

To make analytical progress, we start by noting that within the linear theory, the "compressibility" term $\kappa_1 \nabla_\perp \delta\rho$ and the advective term $\lambda_g \partial_x \delta\mathbf{g} \equiv \lambda_1 g_0 \partial_x \delta\mathbf{g}$ are expected to diverge as $k \to 0$, on account of their scaling dimensions based on both linear and nonlinear analyses. We can therefore approximate the flow equations by assuming the divergence of these terms (or more specifically their dimensionless versions: $\bar{\kappa}_1 = \kappa_1 \gamma/\mu_\perp^2 k^2$ and $\bar{\lambda}_g = \lambda_g/\sqrt{\mu_\perp \mu_x} k$) [25]. Taking this limit, some of the graphical corrections (for λ_1, D, and λ_g) vanish, while others (λ_2, λ_3, $\mu_\perp$, and $\mu_\perp^L$) become finite and completely independent of $\bar{\kappa}_1$ and $\bar{\lambda}_g$ [25].

Unexpectedly, different behavior is observed for the graphical corrections of μ_x,

$$\eta_x = \frac{2D}{2(d-2)\mu_x} \frac{\partial^2}{\partial q_x^2} \int_{\tilde{\mathbf{h}}} \mathcal{P}_{T,ij}(\mathbf{q}) V_{imk}(\mathbf{q},\mathbf{h}) G_{ma}(\tilde{\mathbf{h}}) \times G_{an}(-\tilde{\mathbf{h}}) V_{lnj}(\mathbf{q}-\mathbf{h},-\mathbf{h}) G_{kl}(\tilde{\mathbf{q}}-\tilde{\mathbf{h}}) \delta(h^\perp - k)\Big|_{\tilde{\mathbf{q}}=0} \equiv F_x(\bar{\lambda}_1, \bar{\lambda}_2, \bar{\lambda}_3, \bar{g}_0, \bar{\kappa}_1), \tag{20}$$

where $\int_{\tilde{\mathbf{h}}} d^d h d\omega_h/(2\pi)^{(d+1)}$ and V_{imk} is the three-point momentum density vertex and the $\bar{\lambda}$'s are the dimensionless versions of the λ's (shown in Ref. [25]). First, contrary to the other corrections, the limit of large $\bar{\kappa}_1$ and $\bar{\lambda}_g$ does not commute with the integral over h_x in Eq. (20). If the limit is performed before the integral, one would incorrectly conclude that this correction vanishes. Evaluated in the correct order however, we find via numerical evaluation of Eq. (20) that, as both $\bar{\kappa}_1$ and $\bar{\lambda}_g$ diverge, and $\bar{\lambda}_1$, $\bar{\lambda}_2$ and $\bar{\lambda}_3$ approach a fixed point value (marked by an asterisk), the function F_x behaves asymptotically as

$$F_x(\bar{\lambda}_1, \bar{\lambda}_2, \bar{\lambda}_3, \bar{\lambda}_g, \bar{\kappa}_1) \to \bar{F}_x\left(\bar{\lambda}_1^*, \bar{\lambda}_2^*, \bar{\lambda}_3^*, \frac{\bar{\lambda}_g^{13}}{\bar{\kappa}_1^7}\right), \tag{21}$$

where asterisks denote fixed point values and $\bar{F}_x$ has the asymptotic properties, $\bar{F}_x(\bar{\lambda}_1, \bar{\lambda}_2, \bar{\lambda}_3, 0) = 0$ and $\lim_{x\to\infty} \bar{F}_x(\bar{\lambda}_1, \bar{\lambda}_2, \bar{\lambda}_3, x) = \infty$ [25]. The flow equations therefore only allow a fixed point for two possible scenarios. Either $\bar{\kappa}_1$ tends to infinity fast enough such that $\bar{\lambda}_g^{13} \ll \bar{\kappa}_1^7$, in which case $F_x = \eta_x = 0$ and the TT UC is recovered, or $\bar{\kappa}_1$ and $\bar{\lambda}_g$ diverge in such a way that the ratio $\bar{\lambda}_g^{13}/\bar{\kappa}_1^7$ approaches a constant value, leading to the new UC uncovered here. Specifically, since neither $\bar{\lambda}_g$ nor $\bar{\kappa}_1$ receive any graphical corrections in this limit, using the standard rescaling, we can write down an effective flow equation for $\bar{\lambda}_\kappa = \bar{\lambda}_g^{13}/\bar{\kappa}_1^7$:

$$\partial_l \bar{\lambda}_\kappa = [13(z-\zeta) - 7(2z-2)]\bar{\lambda}_\kappa, \tag{22}$$

with precisely two fixed points: either $\bar{\lambda}_\kappa = 0$ or $\bar{\lambda}_\kappa = \text{const.}$ In the latter case, the exponents have to fulfill the hyperscaling relation

$$13(z-\zeta) - 7(2z-2) = 0. \tag{23}$$

Together with the scaling relations from the vanishing graphical corrections for λ_1 and D (also obtained in Refs. [2,15]):

$$\partial_l \log \bar{\lambda}_1 = z - 1 + \chi = 0, \tag{24}$$

$$\partial_l \log D = z - 2\chi - \zeta - (d-1) = 0, \tag{25}$$

we can determine the analytical expressions of the exponents in Eq. (2). Further, our calculation here applies below $d \sim 2.4$, thus potentially enabling us to extrapolate our numerical FRG results to $d = 2$.

Since the exponents are determined by the various scaling relations and therefore independent of the exact locations of the fixed points, we believe them to be robust against approximations. Indeed, *exact* exponents have been claimed for diverse systems based on scaling relations [2,18,24,34–37]. Further testing the *exactness* of the exponents (2), via simulation or numerical FRG methods, will thus be of great interest.

Finally, we can support the scenario regarding the exchange of stabilities between the TT UC and our novel UC (Fig. 2) by expanding Eq. (22) around the TT fixed point at $\bar{\lambda}_\kappa = 0$,

$$\partial_l \delta\lambda_\kappa = (11 - 3d)\delta\lambda_\kappa, \tag{26}$$

which clearly becomes unstable below $d < d_c' = 11/3$. Further supporting evidence is that the exponents of both the TT UC (17) and our UC (2) coincide at $d = 11/3$, as expected from such an exchange of fixed point stabilities.

Summary and outlook—The Vicsek model together with the Toner-Tu theoretical formulation of polar active fluids helped propel active matter physics into a well-known discipline of physics today, and along the way inspired diverse variations of flocking models that are found to correspond to many novel UCs [18–20,37–45]. Ironically, the UC that governs Vicsek's original flocking phase has remained unknown, perhaps until now. Besides potentially explaining the universal flocking behavior of the Vicsek model, our nonperturbative, FRG calculation may also refute the recent questioning of the stability of the flocking phase [46,47] in $d = 2$, 3, at least when the active systems are deep enough in the ordered phase.

Looking forward, the RG has traditionally been perceived as merely a conceptual way to elucidating the underlying physics [48]; in contrast, our work shows that RG methodology can quantify physical properties accurately, thus demonstrating the power of the RG not readily appreciated. Indeed, FRG methodology has already been used in several other disciplines of physics to provide quantitatively accurate predictions of both universal and nonuniversal quantities [13]. We believe that similar developments in active matter physics will be very fruitful.

Note added—Recently, two other papers have appeared addressing the universality class of the Vicsek model, yielding scaling exponents similar to but distinct from ours [49,50]. In Ref. [49] the mass density as a hydrodynamic variable is neglected and graphical corrections of the nonlinear terms are assumed to vanish, which we believe to be unjustified assumptions. The results of Ref. [50] are based on the assumption that all nonlinearities of the EOM must be total derivatives which we also believe is unjustified (see also footnote [29] of Ref. [51]).

[1] T. Vicsek, A. Czirók, E. Ben-Jacob, I. Cohen, and O. Shochet, Novel type of phase transition in a system of self-driven particles, Phys. Rev. Lett. **75**, 1226 (1995).

[2] J. Toner and Y. Tu, Long-range order in a two-dimensional dynamical XY model: How birds fly together, Phys. Rev. Lett. **75**, 4326 (1995).

[3] G. Grégoire and H. Chaté, Onset of collective and cohesive motion, Phys. Rev. Lett. **92**, 025702 (2004).

[4] J. Toner, Reanalysis of the hydrodynamic theory of fluid, polar-ordered flocks, Phys. Rev. E **86**, 031918 (2012).

[5] B. Mahault, F. Ginelli, and H. Chaté, Quantitative assessment of the Toner and Tu theory of polar flocks, Phys. Rev. Lett. **123**, 218001 (2019).

[6] The FRG is sometimes also called nonperturbative RG (NPRG) or exact RG. While it is sometimes advocated that the name FRG should only be used when the ansatz for the effective action contains functional couplings, and NPRG only when nonperturbative effects are taken into account, we use the term FRG here simply to refer to an approach based on the Wetterich equation (14), even though our ansatz has no functional couplings but still contains nonperturbative effects.

[7] C. Wetterich, Exact evolution equation for the effective potential, Phys. Lett. B **301**, 90 (1993).

[8] T. R. Morris, The exact renormalization group and approximate solutions, Int. J. Mod. Phys. A **09**, 2411 (1994).

[9] U. Ellwanger, Flow equations for N point functions and bound states, Z. Phys. C Part. Fields **62**, 503 (1994).

[10] J. Berges, N. Tetradis, and C. Wetterich, Non-perturbative renormalization flow in quantum field theory and statistical physics, Phys. Rep. **363**, 223 (2002).

[11] P. Kopietz, L. Bartosch, and F. Schütz, *Introduction to the Functional Renormalization Group*, Lecture Notes in Physics Vol. 798 (Springer Berlin Heidelberg, Berlin, Heidelberg, 2010), 10.1007/978-3-642-05094-7.

[12] B. Delamotte, An introduction to the nonperturbative renormalization group, in *Renormalization Group and Effective Field Theory Approaches to Many-Body Systems*, Lecture Notes in Physics, edited by A. Schwenk and J. Polonyi (Springer, Berlin, Heidelberg, 2012), pp. 49–132, 10.1007/978-3-642-27320-9_2.

[13] N. Dupuis, L. Canet, A. Eichhorn, W. Metzner, J. M. Pawlowski, M. Tissier, and N. Wschebor, The nonperturbative functional renormalization group and its applications, Phys. Rep. **910**, 1 (2021).

[14] L. Canet, H. Chaté, and B. Delamotte, General framework of the non-perturbative renormalization group for non-equilibrium steady states, J. Phys. A **44**, 495001 (2011).

[15] J. Toner and Y. Tu, Flocks, herds, and schools: A quantitative theory of flocking, Phys. Rev. E **58**, 4828 (1998).

[16] L. Chen, C. F. Lee, and J. Toner, Mapping two-dimensional polar active fluids to two-dimensional soap and one-dimensional sandblasting, Nat. Commun. **7**, 12215 (2016).

[17] L. Chen, C. F. Lee, A. Maitra, and J. Toner, Dynamics of packed swarms: Time-displaced correlators of two-dimensional incompressible flocks, Phys. Rev. E **109**, L012601 (2024).

[18] L. Chen, C. F. Lee, and J. Toner, Incompressible polar active fluids in the moving phase in dimensions $d > 2$, New J. Phys. **20**, 113035 (2018).

[19] J. Toner, Birth, death, and flight: A theory of Malthusian flocks, Phys. Rev. Lett. **108**, 088102 (2012).

[20] L. Chen, C. F. Lee, and J. Toner, Moving, reproducing, and dying beyond flatland: Malthusian flocks in dimensions $d > 2$, Phys. Rev. Lett. **125**, 098003 (2020).

[21] K. G. Wilson and J. Kogut, The renormalization group and the ϵ expansion, Phys. Rep. **12**, 75 (1974).

[22] E. Brézin and J. Zinn-Justin, Renormalization of the nonlinear σ model in $2+\epsilon$ dimensions—application to the Heisenberg ferromagnets, Phys. Rev. Lett. **36**, 691 (1976).

[23] N. Dupuis, Infrared behavior in systems with a broken continuous symmetry: Classical O(n) model versus interacting bosons, Phys. Rev. E **83**, 031120 (2011).

[24] P. Jentsch and C. F. Lee, Can exact scaling exponents be obtained using the renormalization group? Affirmative evidence from incompressible polar active fluids, arXiv:2307.06725.

[25] See Supplemental Material at http://link.aps.org/supplemental/10.1103/PhysRevLett.133.128301 for further analytical and numerical details.

[26] M. Galassi, J. Davies, J. Theiler, B. Gough, G. Jungman, P. Alken, M. Booth, and F. Rossi, *GNU Scientific Library Reference Manual* (3rd ed.) (Network Theory Ltd, Bristol, 2009).

[27] D. Forster, D. R. Nelson, and M. J. Stephen, Large-distance and long-time properties of a randomly stirred fluid, Phys. Rev. A **16**, 732 (1977).

[28] P. C. Martin, E. D. Siggia, and H. A. Rose, Statistical dynamics of classical systems, Phys. Rev. A **8**, 423 (1973).

[29] C. De Dominicis, Techniques de renormalisation de la théorie des champs et dynamique des phénomènes critiques, Le J. Phys. Colloq. **37**, C1 (1976).

[30] H.-K. Janssen, On a Lagrangean for classical field dynamics and renormalization group calculations of dynamical critical properties, Z. Phys. B Condens. Matter **23**, 377 (1976).
[31] L. Canet, B. Delamotte, and N. Wschebor, Fully developed isotropic turbulence: Symmetries and exact identities, Phys. Rev. E **91**, 053004 (2015).
[32] P. Jentsch and C. F. Lee, Critical phenomena in compressible polar active fluids: Dynamical and functional renormalization group studies, Phys. Rev. Res. **5**, 023061 (2023).
[33] T. R. Morris, Momentum scale expansion of sharp cutoff flow equations, Nucl. Phys. **B458**, 477 (1996).
[34] T. Hwa and M. Kardar, Dissipative transport in open systems: An investigation of self-organized criticality, Phys. Rev. Lett. **62**, 1813 (1989).
[35] J. Toner, N. Guttenberg, and Y. Tu, Swarming in the dirt: Ordered flocks with quenched disorder, Phys. Rev. Lett. **121**, 248002 (2018).
[36] S. Mahdisoltani, R. B. A. Zinati, C. Duclut, A. Gambassi, and R. Golestanian, Nonequilibrium polarity-induced chemotaxis: Emergent galilean symmetry and exact scaling exponents, Phys. Rev. Res. **3**, 013100 (2021).
[37] L. Chen, C. F. Lee, A. Maitra, and J. Toner, Packed swarms on dirt: Two-dimensional incompressible flocks with quenched and annealed disorder, Phys. Rev. Lett. **129**, 188004 (2022).
[38] L. Chen, J. Toner, and C. F. Lee, Critical phenomenon of the order–disorder transition in incompressible active fluids, New J. Phys. **17**, 042002 (2015).
[39] L. Chen, C. F. Lee, and J. Toner, Squeezed in three dimensions, moving in two: Hydrodynamic theory of three-dimensional incompressible easy-plane polar active fluids, Phys. Rev. E **98**, 040602(R) (2018).
[40] J. Toner, N. Guttenberg, and Y. Tu, Hydrodynamic theory of flocking in the presence of quenched disorder, Phys. Rev. E **98**, 062604 (2018).
[41] L. Chen, C. F. Lee, and J. Toner, Universality class for a nonequilibrium state of matter: A $d = 4 - \epsilon$ expansion study of Malthusian flocks, Phys. Rev. E **102**, 022610 (2020).
[42] L. Chen, C. F. Lee, A. Maitra, and J. Toner, Hydrodynamic theory of two-dimensional incompressible polar active fluids with quenched and annealed disorder, Phys. Rev. E **106**, 044608 (2022).
[43] L. Chen, C. F. Lee, A. Maitra, and J. Toner, Incompressible polar active fluids with quenched random field disorder in dimensions $d > 2$, Phys. Rev. Lett. **129**, 198001 (2022).
[44] R. B. A. Zinati, M. Besse, G. Tarjus, and M. Tissier, Dense polar active fluids in a disordered environment, Phys. Rev. E **105**, 064605 (2022).
[45] A. Cavagna, L. Di Carlo, I. Giardina, T. S. Grigera, S. Melillo, L. Parisi, G. Pisegna, and M. Scandolo, Natural swarms in 3.99 dimensions, Nat. Phys. **19**, 1043 (2023).
[46] J. Codina, B. Mahault, H. Chaté, J. Dobnikar, I. Pagonabarraga, and X. Q. Shi, Small obstacle in a large polar flock, Phys. Rev. Lett. **128**, 218001 (2022).
[47] B. Benvegnen, O. Granek, S. Ro, R. Yaacoby, H. Chaté, Y. Kafri, D. Mukamel, A. Solon, and J. Tailleur, Metastability of discrete-symmetry flocks, Phys. Rev. Lett. **131**, 218301 (2023).
[48] J. Cardy, *Scaling and Renormalization in Statistical Physics* (Cambridge University Press, Cambridge, 1996).
[49] The original result was presented in H. Ikeda, Scaling theory of continuous symmetry breaking under advection, arXiv:2401.01603 and a simplified version was later presented in Minimum scaling model and exact exponents for the Nambu-Goldstone modes in the Vicsek model, arXiv:2403.02086.
[50] H. Chaté and A. Solon, Dynamic scaling of two-dimensional polar flocks, Phys. Rev. Lett. **132**, 268302 (2024).
[51] J. Toner, Birth, death, and horizontal flight: Malthusian flocks with an easy plane in three dimensions, arXiv:2407.03071.